Weld World (2015) 59:655–665
DOI 10.1007/s40194-015-0241-4

RESEARCH PAPER

Dissimilar welding of the creep resistant steels CB2 and P92 with flux cored wires

S. Baumgartner · M. Schuler · A. Holy · R. Schnitzer · N. Enzinger

Received: 2 October 2014 / Accepted: 4 March 2015 / Published online: 21 March 2015

Abstract The new boron-alloyed 9Cr-1.5Mo-1Co cast steel designated as CB2 is used for intermediate pressure turbine inner casings with steam temperature up to 620 °C. To connect the casing with a pipe made of P92 steel, dissimilar welding is necessary. As flux cored arc welding (FCAW) is a highly productive welding process, the applicability of flux cored wires is evaluated. Therefore, three test welds in vertical-up position were produced with different welding procedures: the first with P92 tungsten inert gas (TIG) welding for root and second pass and P92 FCAW for intermediate and final passes; the second with P92 TIG welding for root and second pass and CB2 FCAW for intermediate and final passes; and the third with CB2 flux cored wire for all layers as no CB2 TIG rod is available yet. Cross-weld tensile tests and impact tests on weld metal and heat-affected zones were carried out after post weld heat treatment (PWHT) of 2×730 °C for 12 h. The differences in mechanical and technological properties are discussed, as well as the hardness profiles in the cross sections. Thermokinetic calculations with the software package MatCalc estimate the long-term microstructural evolution of precipitates depending on the chemical composition of the weld metal.

Doc. IIW-2553, recommended for publication by Commission IX "Behaviour of Metals Subjected to Welding"

S. Baumgartner (✉) · A. Holy · R. Schnitzer
voestalpine Böhler Welding Austria GmbH, Böhler-Welding-Straße 1, 8605 Kapfenberg, Austria
e-mail: Susanne.Baumgartner@voestalpine.com

M. Schuler · N. Enzinger
Institute for Materials Science and Welding, Graz University of Technology, Kopernikusgasse 24, 8010 Graz, Austria

Keywords (IIW Thesaurus) Creep resisting materials · Cored filler wire · GMA welding · Welded joints · Mechanical properties

1 Introduction

The boron-alloyed 9Cr-1.5Mo-1Co cast steel called CB2 (see Table 1) was developed and qualified in the European research programs COST501/III to COST536 (1993–2009).

Long-term creep tests exceeding 130,000 h confirm the improved creep rupture strength of CB2 up to 650 °C, which is provided by finely dispersed MX particles and boron-stabilized $M_{23}C_6$ particles. It has already been used for cast components such as turbine casings and valve bodies with operating temperatures up to 620 °C [2]. Figure 1 shows one part of an industrial scale intermediate pressure (IP) inner casing with a delivery weight of approx 35 t of each part made of CB2 and manufactured at voestalpine foundry Linz [3].

As welding is an important part of the production process of large cast components, the development of matching filler metals started parallel to the development of the base material [4]. FCAW provides several technical and economic advantages and especially flux cored wires with a rutile slag system show very good out of position weldability, easy handling, and high productivity [5]. The demand for highly productive welding processes forced the development of a matching flux cored wire, which has already been qualified for welding thick components [3].

Dissimilar welding of CB2 cast components to P92 pipes can either be performed with the co-containing CB2 matching filler metal or with W-alloyed P92 welding consumables. To evaluate the usability of rutile based flux cored wires, pretests on 20 mm plates were performed in vertical-up position.

Table 1 Chemical composition of 9Cr-1.5Mo-1Co cast steel CB2 in wt% [1]

C	Mn	Cr	Mo	Co	Ni	V	Nb	N	B
0.12	0.88	9.20	1.49	0.98	0.17	0.21	0.06	0.020	0.011

2 Experimental procedure

Three dissimilar joints were produced with different filler metal. For variants I and II, root pass and second pass were TIG welded with P92 rods. Intermediate and final passes were welded with flux cored wire, matching to P92 in variant I and matching to CB2 in variant II. As no CB2 TIG rod is available yet, the CB2 flux cored wire was used for root pass, intermediate and final passes of variant I. Although it is unusual and not recommended to use the flux cored wire for root welding, it has been proven for a matching joint of CB2 that it is generally possible [6].

2.1 Welding parameters of dissimilar joints

The seam preparation for all three welds is shown in Fig. 2, and the welding parameters are listed in Table 2.

2.2 Base material

Fig. 1 CB2 IP inner casing manufactured at voestalpine foundry Linz [3]

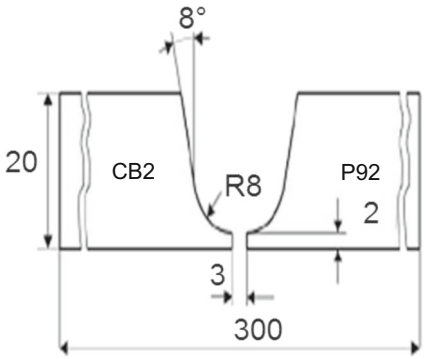

Fig. 2 Seam preparation for dissimilar joints of CB2 and P92

Chemical composition and mechanical properties of base material P92 [7] and CB2 [3] are given in Tables 3 and 4, respectively.

2.3 Filler metal

2.3.1 P92 TIG rod

The P92 TIG rod was especially designed for the welding of P92 and is approved in long-term condition up to 650 °C

Table 2 Welding parameters and PWHT for dissimilar joints of CB2 and P92

	I	II	III
Root pass and second pass	P92 TIG	P92 TIG	CB2 FCW
Diameter [mm]	2.4	2.4	1.2
Current [A]	105	105	115
Voltage [V]	13	13	19
Feeding rate [m/min]			5.4
Heat input [kJ/mm]	1.4	1.4	0.9
Intermediate and final passes	P92 FCW	CB2 FCW	CB2 FCW
Diameter [mm]	1.2	1.2	1.2
Current [A]	173	173	173
Voltage [V]	24	24	24
Feeding rate [m/min]	7.3	7.3	7.3
Heat input [kJ/mm]	1.2	1.2	1.2
Position	PF (3G)		
Shielding gas TIG	Ar		
Shielding gas FCAW	Ar+18 % CO2		
Preheating	150 °C		
Interpass temp.	150 °C		
Welding speed FCW	20 cm/min		
PWHT	2×730 °C/12 h		

Table 3 Measured chemical composition of the base material [wt%]

	C	Mn	P	S	Si	Cr	Ni	Mo	V	W	Co	Nb	Al	Ti	N	B
P92	0.10	0.42	0.019	0.0004	0.26	8.81	0.11	0.31	0.19	1.62	–	0.072	0.040	0.002	0.036	0.0012
CB2	0.13	0.84			0.27	9.10	0.15	1.50	0.20	–	0.98	0.074	0.013		0.027	0.0110

service temperature. The typical chemical composition of the P92 TIG rod and the mechanical properties of all-weld metal according to the product data sheet are listed in Tables 5 and 6, respectively [8].

2.3.2 P92 flux cored wire

The P92 flux cored wire has already been available for several years. The chemical composition of the weld metal used to be close to the chemical composition of the base material. Since 2012, it has been standardized according to AWS A5.36/A5.36 M. The limits of the standard and additional customer requests of Mn + Ni <1.2 wt% necessitated the modification of the chemical composition of all-weld metal to meet these requirements. Table 7 shows the limits of the chemical composition according to the standard and typical values of all-weld metal welded with shielding gas Ar +18 % CO_2. Tension test requirements and mechanical properties of all-weld metal at ambient temperature after PWHT of 760 °C/4 h are given in Table 8.

The mechanical properties of P92 flux cored wire weld metal are strongly influenced by PWHT (see Figs. 3 and 4). By increasing the annealing time from 760 °C/2 h, acc. to AWS A5.36 to 760 °C/4 h tensile properties are slightly lower, but impact toughness is clearly improved. Therefore, a PWHT of 760 °C for 4 h is recommended for the P92 flux cored wire for matching joints [9]. A relatively low annealing temperature of 730 °C is commonly used for cast components. Therefore, the annealing time has to be increased to ensure good toughness properties at ambient temperature.

Table 4 Mechanical properties of the base material at ambient temperature

	Y.S. [MPa]	T.S. [MPa]	El. [%]	CVN at +20 °C [J]
P92	591	739	27	
CB2	561	712	17	36

2.3.3 CB2 flux cored wire

As FCAW provides technical and economic advantages, a matching flux cored wire for welding the newly developed cast steel CB2 has been developed. It is based on the rutile/basic slag system of the already available 9 % Cr flux cored wires for welding P91 and P92. The chemical composition of all-weld metal was kept close to the chemical composition of the base material. Due to the detrimental influence of high boron contents on hot cracking susceptibility and impact toughness, care was taken in an appropriate adjustment of the boron content [6]. The Ni content was kept in the range of the base metal, as Ni is known to be detrimental for long-term properties of 9 % Cr steels [10]. The typical chemical composition of the all-weld metal and the mechanical properties at ambient temperature with a PWHT of 730 °C/24 h are shown in Tables 9 and 10, respectively.

The CB2 flux cored wire has already been tested in a matching joint [6], the results of cross-weld tensile tests and impact tests are given in Table 11.

2.4 Testing program

After X-ray examination, samples were produced to perform side bend tests, cross tensile tests, and impact tests at ambient temperature, and cross sections were taken for light optical metallography (LOM) and hardness measurement.

2.5 Simulation of microstructure evolution with MatCalc

To estimate the long-term creep properties of the dissimilar joints, calculations with the thermokinetic software package

Table 5 Typical chemical composition of P92 TIG rod [wt%]

C	Si	Mn	Cr	Ni	Mo	V	Nb	W	N
0.10	0.3	0.5	8.6	0.5	0.4	0.2	0.05	1.5	0.04

Table 6 Mechanical properties of all-weld metal P92 TIG rod after PWHT 760 °C/6 h

	RT	650 °C
Y.S. [MPa]	650	230
UTS [MPa]	770	340
El. [%]	20	21
CVN [J]	70	

Table 8 Tension test requirements acc. to AWS A5.36 M and typical values of P92 flux cored wire weld metal at ambient temperature

	Minimum	Maximum	FCW
Y. S. [MPa]	540		580
T. S. [MPa]	620	760	730
El. [%]	17		18

MatCalc [11] were carried out for weld metal and heat-affected zone (HAZ) of CB2 and P92, respectively, using the databases mc_fe_v2.019.tdb and mc_fe_v2.005.ddb. The chemical composition of the base material was used according to Table 3 and of all-weld metal according to Tables 7 and 9, respectively. The applied thermal cycle for the P92 base material was normalizing at 1050 °C for 1 min/mm and annealing at 770 °C for 3 min/mm according to the material datasheet [7]. To simulate the temperature effect of multilayer welding, a temperature profile with peak temperatures of 1300, 1000, and 750 °C, respectively, and a $t_{8/5}$ of 12 s for every cycle with interpass temperature of 150 °C was used. Figure 5 shows the temperature cycle schematically for the HAZ using the example of CB2, which consists of casting, welding, PWHT of 2×730 °C for 12 h, and service at 625 °C for 100,000 h.

The evolution of precipitates was simulated for CB2 and P92 weld metal and HAZ, respectively, and phase fraction, mean radius, and number density of the precipitates were calculated. To evaluate the results of the calculation, the calculated values of phase fraction and mean radius of laves phase were compared to the experimental values measured in a CB2 all-weld metal creep specimen, which fractured after 6572 h at 625 °C [12].

Transmission electron microscope (TEM) investigations of CB2 weld metal in as-welded condition revealed the presence of Cr carbides due to the annealing effect of multilayer welding (see Fig. 6). To consider this fact, the MatCalc simulation has been modified to a welding cycle with three peak temperatures.

Table 7 Requirements of chemical composition acc. to AWS A5.36/A5.36 M and typical values of all-weld metal [wt%]

	Minimum	Maximum	Typical values
C	0.08	0.15	0.1
Si		0.50	0.2
Mn		1.20	0.7
P		0.020	
S		0.015	
Cr	8.0	10.0	8.5
Mo	0.30	0.70	0.5
Ni		0.80	0.4
Nb	0.02	0.08	0.04
N	0.02	0.08	0.04
V	0.15	0.30	0.2
W	1.50	2.00	1.5
Al		0.04	
Cu		0.25	
B		0.006	
Co	To be reported if intentionally added		
Mn + Ni		1.40	<1.2

3 Results

All three welded joints passed the X-ray examination, as no non-acceptable defects were detected.

3.1 Side bend tests

All side bend tests acc. to EN ISO 5173 with a mandrel diameter of 40 mm could be performed to an angle of 180° without cracks (see Fig. 7).

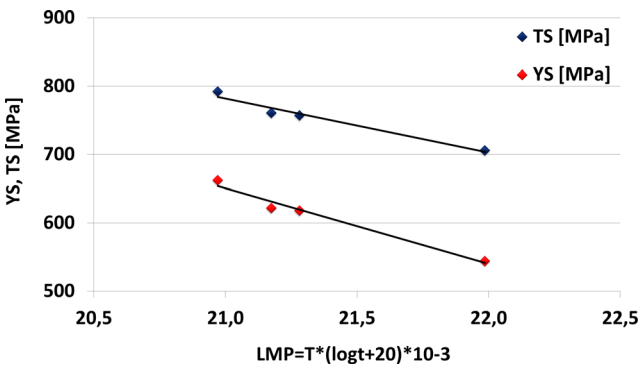

Fig. 3 Influence of PWHT on tensile properties of P92 flux cored wire weld metal at ambient temperature

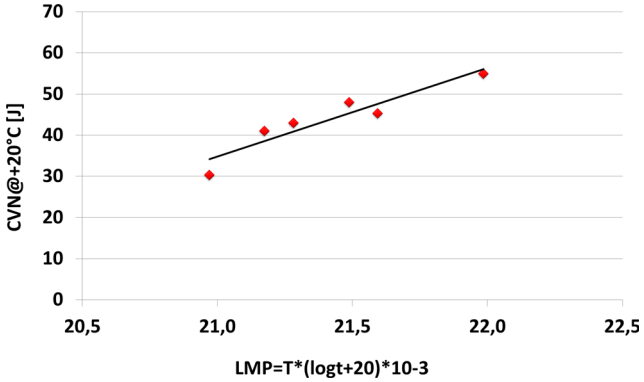

Fig. 4 Influence of PWHT on impact energy of P92 flux cored wire weld metal at ambient temperature

3.2 Mechanical properties of dissimilar joints

3.2.1 Cross-weld tensile tests

Cross-weld tensile tests acc. to EN ISO 4136 were performed, and all specimens fractured outside the weld metal (WM) on the CB2 side (see Fig. 8). Figure 9 reveals that the fracture occurred in the base material.

3.2.2 Impact tests

Figure 10 shows the results of impact tests acc. to EN ISO 9016 of weld metal and HAZ at ambient temperature. The HAZ of P92 shows the highest impact energy, as expected. The values of the weld metal are slightly lower than the values of the HAZ of CB2. Variant II with the combination of P92 TIG welding for the root and second pass and CB2 flux cored wire for intermediate and final passes achieves the highest impact values.

3.2.3 Hardness HV10 measurements

Figure 11 shows the HV10 measurements across the dissimilar joints in root and final layers 2 mm from the surface. After PWHT, the hardness of the weld metal is slightly higher than the hardness of the base materials. In HAZ, hardness peaks occur close to the fusion line followed by a hardness drop close to the base material, which are more or less distinctive.

Table 9 Chemical composition of CB2 flux cored wire weld metal [wt%]

C	Si	Mn	Cr	Mo	Co	Ni	V	Nb	N	B
0.12	0.2	0.9	9.0	1.5	1.0	0.2	0.2	0.03	0.02	0.006

Table 10 Mechanical properties of all-weld metal at ambient temperature with PWHT 730 °C/24 h

Y.S. [MPa]	T.S. [MPa]	El. [%]	CVN at RT [J]
590	740	17	30

3.3 Simulation of microstructure evolution with MatCalc

Table 12 lists the calculated results of phase fraction and mean radius of precipitates in CB2 and P92 flux cored wire weld metals after 10,000 and 100,000 h of service at 625 °C. The main phases are Cr carbides, which precipitate during multilayer welding and PWHT, followed by laves phase, which occurs mainly during service. No Z-phase is predicted up to 100,000 h, as expected. Although, there is not much difference between 10.000 and 100,000 h regarding phase fractions, but the mean radius increases significantly. This indicates a reduction in number density in both weld metals. In CB2 weld metal, the phase fraction of $M_{23}C_6$ is higher than the phase fraction in the P92 weld metal, and the mean radius is only slightly higher. The phase fraction of laves phase is also higher with higher mean radius. In P92 weld metal, the MX particles are smaller, and the amount of VN is about twice the amount in the CB2 weld metal, while the amount of NbC is slightly higher.

According to the simulation, boron forms BN in the weld metal, however, in the HAZ, M_2B borides are formed, and VN is unstable in HAZ. Figures 12 and 13 compare the evolution of the main precipitates in CB2 and P92 flux cored wire weld metal at selected times. The empty symbols are for CB2 and the filled symbols are for P92.

Figures 14 and 15 compare the evolution of the main precipitates in the HAZ of CB2 and P92, respectively, at selected times. The empty symbols are again for CB2 and the filled symbols are for P92.

Before welding, the phase fraction of $M_{23}C_6$ is about 3 wt% in CB2 and about 1 wt% in P92. The carbides resolve during welding and renucleate during PWHT. In

Table 11 Cross-weld tensile test results of a CB2-FCAW butt weld at room temperature (RT) and at 650 °C (PWHT 2×730 °C/12 h)

	+20 °C	650 °C
UTS [MPa]	727	342
Fracture location	BM/HAZ	BM/HAZ
CVN at +20 °C [J]	29-37-34	

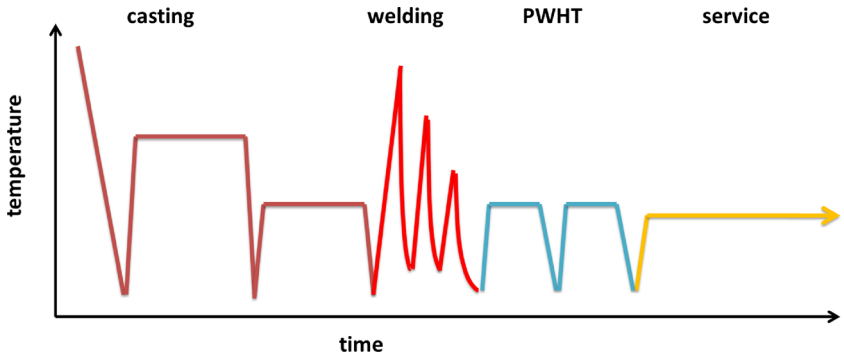

Fig. 5 Temperature profile of CB2 HAZ

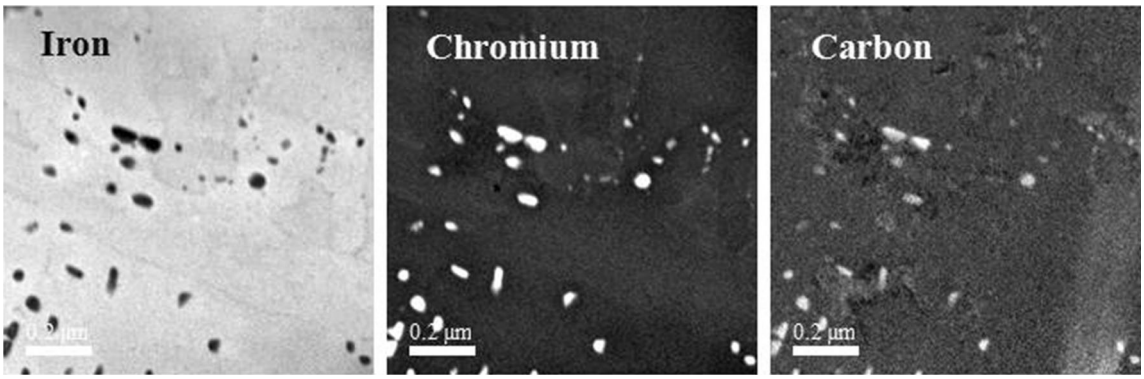

Fig. 6 TEM investigation of CB2 flux cored wire weld metal in as-welded condition

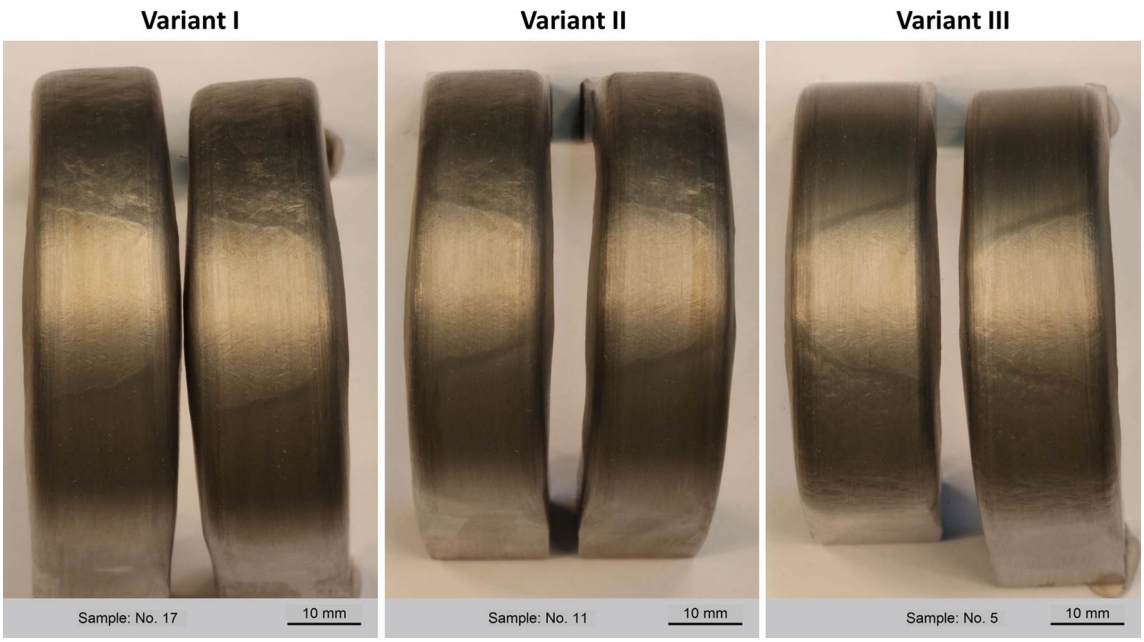

Fig. 7 Side bend test of dissimilar joints

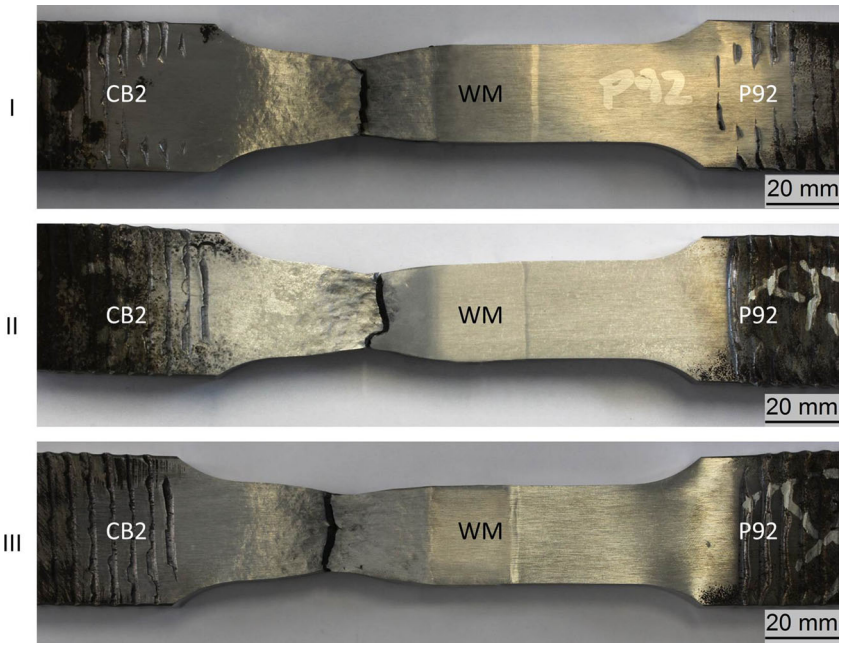

Fig. 8 Fracture location of cross tensile specimen

CB2, the phase fraction stays constant at about 3 wt%; in P92, it increases to about 2 wt%. The precipitates are only slightly coarser in P92 after PWHT, but increase more during service. Laves phase starts to nucleate during PWHT and coarsens during service. The amount of laves phase is slightly higher in CB2, but also the mean radius is higher. The amount of NbC is quite low, but the precipitates stay stable in both materials. The amount of borides is also quite low, but they dramatically coarsen during service.

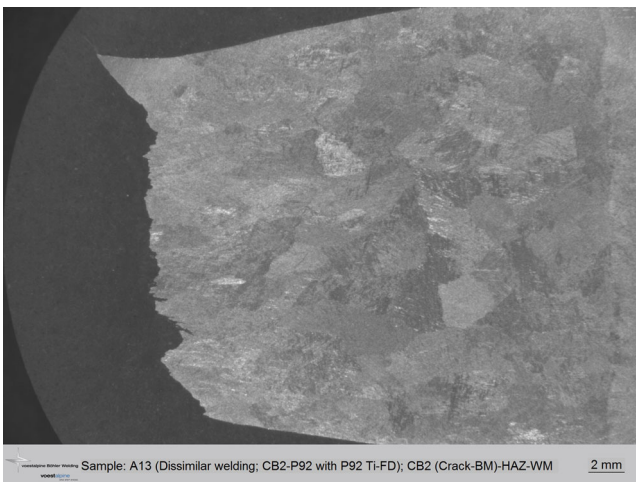

Fig. 9 Fracture location of cross tensile specimen

4 Discussion of results

Basically, the CB2 and the P92 flux cored wire are both suitable for dissimilar welding of CB2 and P92. Cross tension tests and hardness measurements indicate that the weakest part of the joint at ambient temperature is the HAZ of CB2. Regarding the properties of the flux cored wire weld metals, the CB2 flux cored wire shows higher values of impact energy after PWHT of 2× 730 °C/12 h. However, it should be possible to improve the impact energy of P92 flux cored wire weld metal with optimized welding parameters.

Schubert [13] recommends using P92 filler metal for similar and dissimilar joints of CB2 due to higher creep rupture strength, based on the results of similar and dissimilar joints welded with stick electrodes. In the similar joints of CB2, the fracture location always occurred in the weld metal, whereas the samples welded with P92 filler metal showed higher creep rupture strength. In dissimilar joints of CB2 and P92, the fracture occurred in the HAZ of P92. However, samples welded with CB2 filler metal fractured in the weld metal [13].

Creep rupture tests of similar joints welded with the CB2 flux cored wire at 625 °C revealed different results. Weld metal samples performed slightly better than cross-weld samples, which fractured in the base material and the HAZ, respectively. Although, when

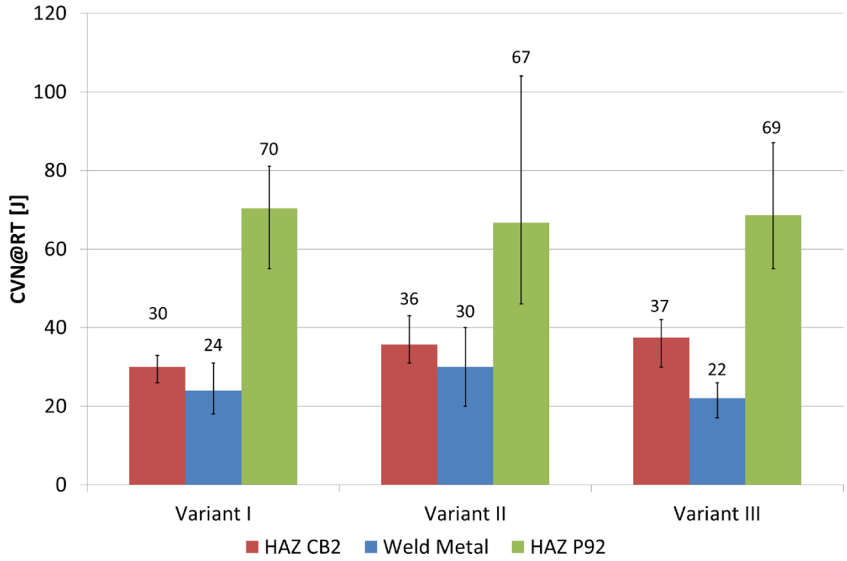

Fig. 10 Impact tests of weld metal and HAZ at ambient temperature

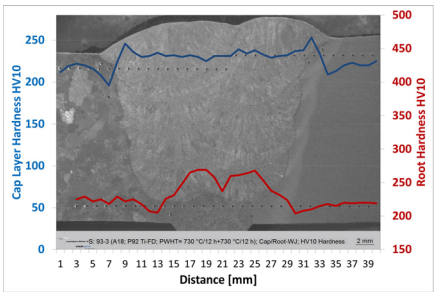

BM CB2	HAZ CB2	WM I	HAZ P92	BM P92
212-222	196-246	225-239	209-253	220-225
218-229	205-274	237-269	204-254	210-220

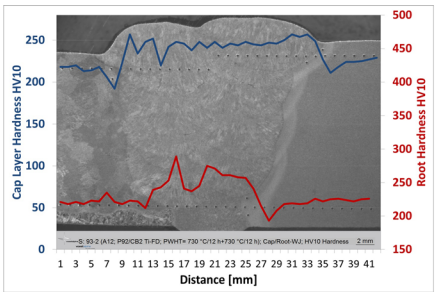

BM CB2	HAZ CB2	WM II	HAZ P92	BM P92
213-220	192-257	220-257	211-257	218-229
218-257	212-289	237-275	193-257	208-226

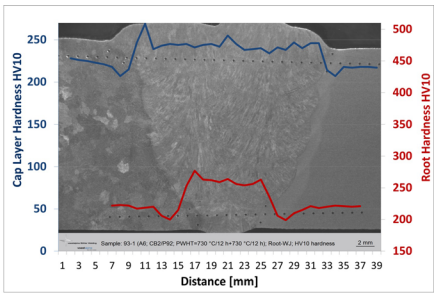

BM CB2	HAZ CB2	WM III	HAZ P92	BM P92
218-228	207-269	234-255	207-246	217-220
217-223	200-277	254-264	199-263	215-222

Fig. 11 Hardness profiles of dissimilar joints

Table 12 Calculated phase fraction [wt%] and mean radius [nm] of precipitates in CB2 and P92 flux cored wire weld metal after 10,000 and 100,000 h of service at 625 °C

Material	CB2—WM				P92—WM			
Phase fraction [wt%], mean radius [nm]	10,000 h		100,000 h		10,000 h		100,000 h	
	wt%	nm	wt%	nm	wt%	nm	wt%	nm
$M_{23}C_6$	2.98	655	2.99	1324	2.17	603	2.19	1193
Laves phase	0.82	453	0.82	1091	0.65	168	0.69	407
VN	0.15	125	0.16	165	0.31	58	0.31	113
NbC	0.03	214	0.02	199	0.02	211	0.02	192
BN	0.04	222	0.04	456	0.03	229	0.03	466

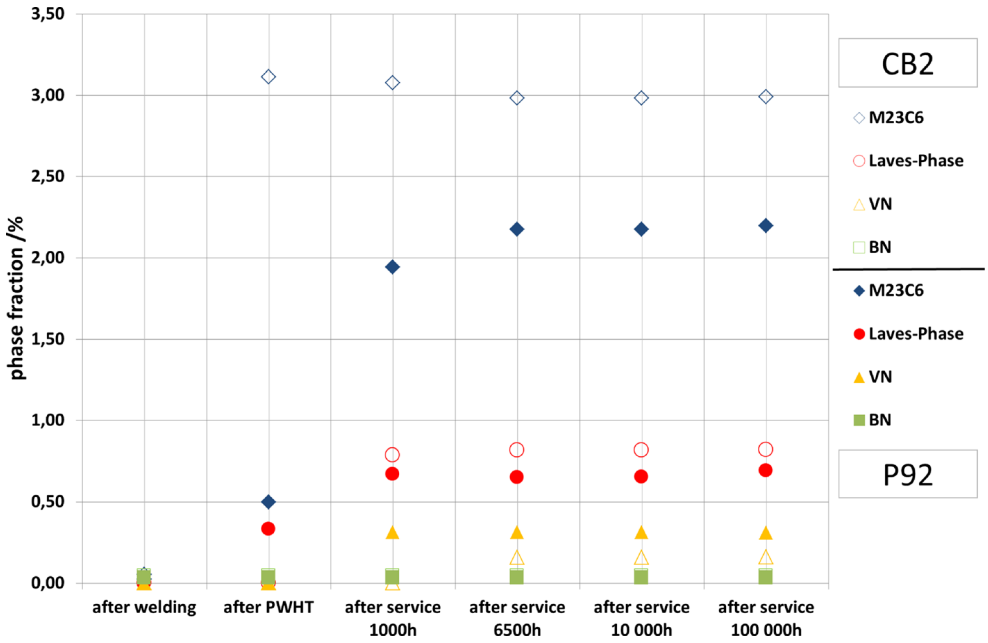

Fig. 12 Evolution of main precipitates in weld metal of CB2 and P92

the results of P92 all-weld metal samples are compared to CB2 flux cored wire weld metal, the P92 flux cored wire reveals higher creep rupture strength at 625 °C (see Fig. 16).

MatCalc simulations show only few differences between CB2 and P92 weld metal. Phase fraction and mean radius of the precipitates are generally in the same range. The amount of $M_{23}C_6$ is higher in the CB2 weld metal, but the amount of MX precipitates (VN and NbC) is significantly higher in the P92 weld metal, which could be interpreted as an indicator for a better creep performance. But the results of the simulation have to be handled cautiously and can only be interpreted as an assumption.

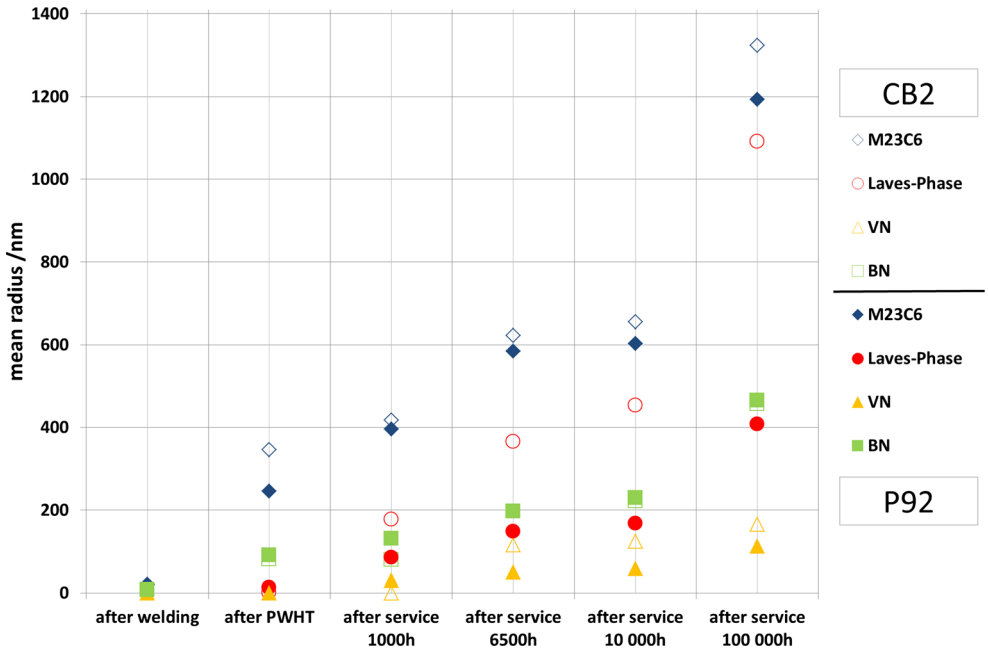

Fig. 13 Evolution of mean radius of precipitates in weld metal of CB2 and P92

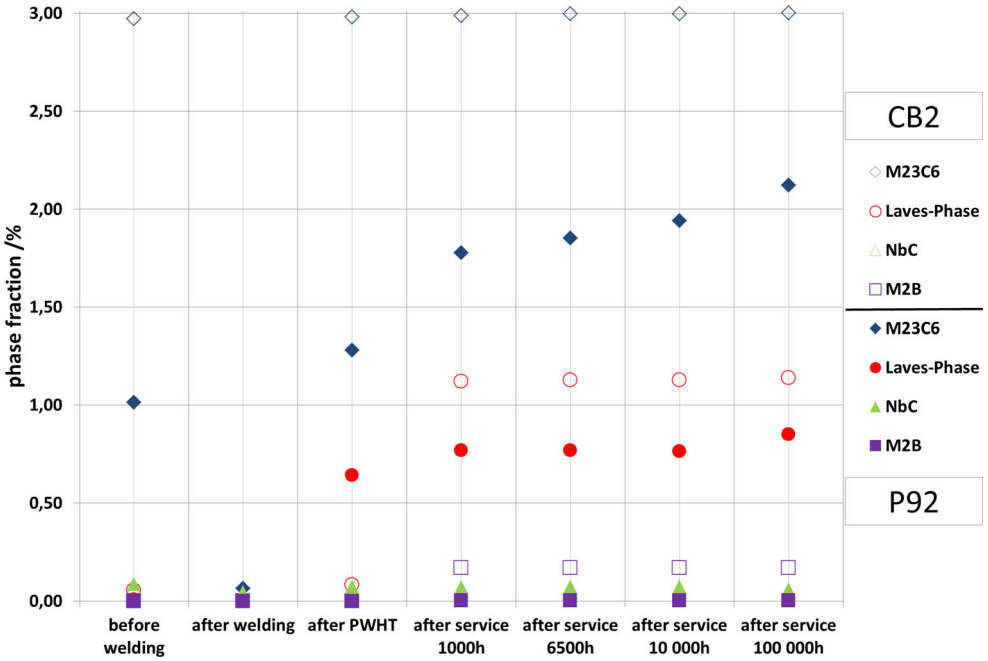

Fig. 14 Evolution of main precipitates in HAZ of CB2 and P92

5 Conclusion

P92 and CB2 flux cored wires were used for dissimilar welding. All cross tensile specimens fractured in the CB2 base material. Hardness measurements indicate that the CB2 HAZ seems to be the weakest zone of the dissimilar joint.

Impact energy at room temperature of CB2 weld metal is slightly higher using TIG welding P92 for root and second

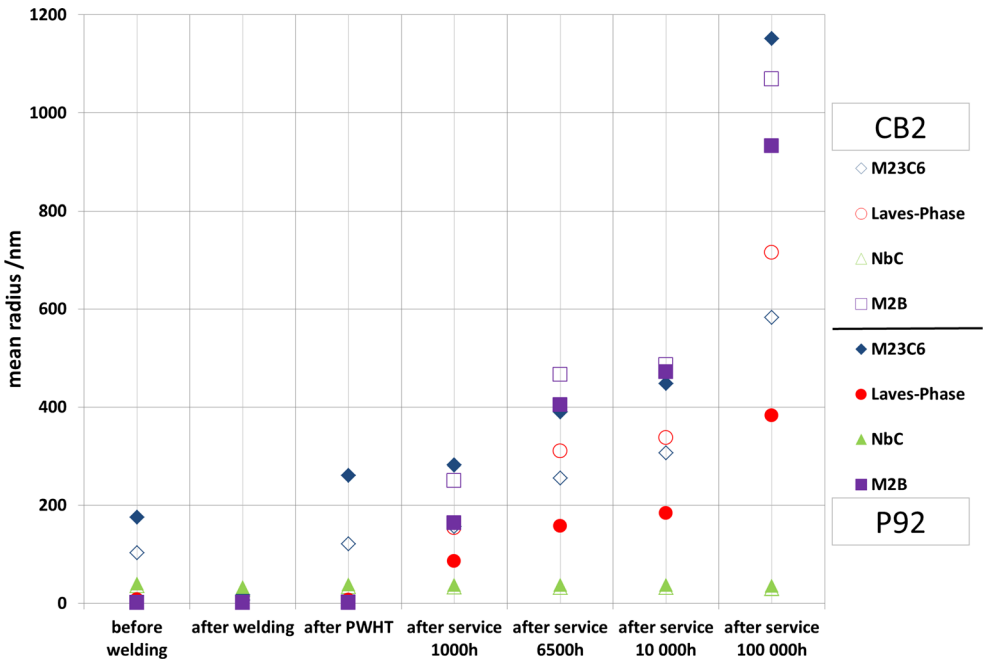

Fig. 15 Evolution of mean radius of precipitates in HAZ of CB2 and P92

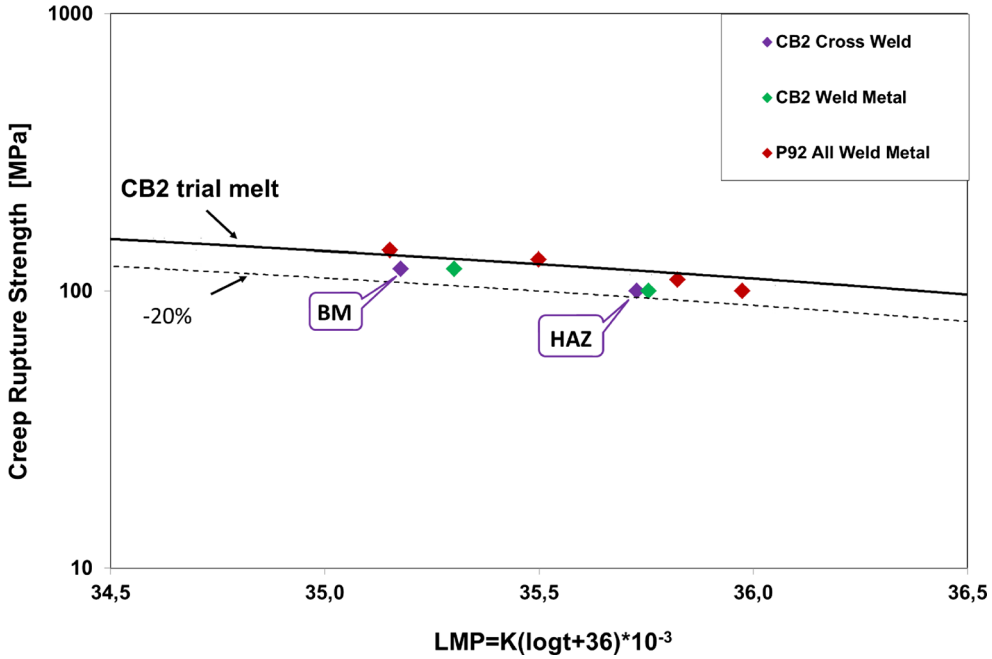

Fig. 16 Creep rupture tests for CB2 and P92 flux cored wires at 625 °C

pass, but at 625 °C the creep rupture strength of P92 weld metal is higher.

MatCalc simulations show only few differences between CB2 and P92 weld metal, and in both cases, no Z-phase occurred according to the calculations.

Acknowledgments The authors want to thank the Austrian "Forschungsförderungsgesellschaft" (FFG) for the financial support based on the contract no. 831995.

References

1. Staubli M, Hanus R, Weber T, Mayer K.-H, Kern T.-U (2006) The European efforts in development of new high temperature casing materials—COST536, Materials for Advanced Power Engineering, Proceedings Part II, pp 855–870
2. Vanstone R, Chilton I, Jaworski P (2013) Manufacturing experience in an advanced 9 %CrMoCoVNbNB alloy for ultra-supercritical steam turbine rotor forgings and castings. J Eng Gas Turbines Power 135
3. Lochbichler C, Schmidtne-Kelity E, Baumgartner S (2013) Latest developments of cast materials and welding consumables for coal-fired steam turbines components/nickel-base alloy A625 and CB2 steel for the A-USC technology, Proceedings of Power Gen, Vienna
4. Bauné E, Cerjak H, Caminada St, Jochum C, Mayr P, Pasternak J (2006) Weldability and properties of new creep resistant materials for use in ultra supercritical coal fired power plants, Materials for Advanced Power Engineering, Proceedings Part II, pp 871–891
5. Posch G, Baumgartner S, Fiedler M (2009) GMA-welding of creep resistant steels with flux cored wires (FCAW): perspectives and limitations, Proceedings of the IIW International Conference on Advances in Welding and Allied Technologies, Singapore 16–17 July, pp 619–624
6. Baumgartner S, Posch G, Mayr P (2012) Welding advanced martensitic creep resistant steels with boron containing filler metal. Weld World 56(7/8), pp 2–9
7. Certificate No. 518950, Industeel, Belgium
8. Product data sheet of Böhler P92-IG, www.voestalpine.com/welding/austria/products
9. Baumgartner S, Schnitzer R, Schuler M, Schmidtne-Kelity E, Lochbichler C (2013) Flux cored wires for welding advanced 9–10 % Cr steels, advances in materials technology for fossil power plants, Proceedings from the Seventh International Conference October 22–25, Waikoloa, Hawaii, USA, pp 936–947
10. Kimura K, Sawada K, Kushima H, Toda Y (2011) Microstructural stability and long-term creep strength of grade 91 steel, energy materials: materials science and engineering for energy systems, Vol. 4, No. 4, 8th Charles Parsons Turbine Conference, pp 176–183
11. http://matcalc.tuwien.ac.at/, Vienna. 2013
12. Baumgartner S, Schuler M, Ramskogler C, Schmidtne-Kelity E, Sarić A, Schnitzer R, Lochbichler C, Enzinger N (2013) Mikrostrukturentwicklung von CB2 Fülldraht-Schweißungen, Tagungsband der 36. Vortragsveranstaltung der Arbeitsgemeinschaft für warmfeste Stähle und Hochtemperaturwerkstoffe in Düsseldorf, 22. November, pp 29–40
13. Schubert J, Schwass G (2012) Zeitstandverhalten von modernen martensitischen Stahlguss-Schweißverbindungen im Temperaturgebiet 550–650°C, Tagungsband der 35. Vortragsveranstaltung der Arbeitsgemeinschaft für warmfeste Stähle und Hochtemperaturwerkstoffe in Düsseldorf, 30. November, pp 22–38